10-2010

Investigation of carbon corrosion in polymer electrolyte fuel cells using steam etching

Mei-xian Wang
Indiana University - Purdue University Indianapolis

Hong-fang Sun
Purdue University - Main Campus

Noma Ogbeifun
Indiana University - Purdue University Indianapolis

Fan Xu
Indiana University - Purdue University Indianapolis

E A. Stach
Birck Nanotechnology Center and School of Materials Engineering, Purdue University, eastach@purdue.edu

See next page for additional authors

Materials Chemistry and Physics 123 (2010) 761–766

Contents lists available at ScienceDirect

Materials Chemistry and Physics

journal homepage: www.elsevier.com/locate/matchemphys

Investigation of carbon corrosion in polymer electrolyte fuel cells using steam etching

Mei-xian Wang[a], Qi Liu[a], Hong-fang Sun[b], Noma Ogbeifun[a], Fan Xu[a], Eric A. Stach[b], Jian Xie[a,*]

[a] Department of Mechanical Engineering, Purdue School of Engineering and Technology, Indiana University-Purdue University, Indianapolis, IN 46202, USA
[b] School of Materials Engineering and Birck Nanotechnology Center, Purdue University, West Lafayette, IN 47907, USA

ARTICLE INFO

Article history:
Received 20 October 2009
Accepted 20 May 2010

Keywords:
Surfaces
Etching
Electron microscopy
Corrosion

ABSTRACT

Carbon blacks are widely used as electrocatalyst supports in polymer electrolyte fuel cells (PEFCs), and the corrosion of carbon blacks has a severe impact on the long-term durability of PEFCs. The steam etching approach was used to investigate the corrosion of the low-surface area XC72 carbon black and the high-surface area black pearl 2000 carbon black under different conditions. The weight loss of the XC72 and the black pearl 2000 when etched at 800 °C for 3 h is 28.43% and 54.82%, respectively. TEM results show that the corrosion of the XC72 begins from the center of the particle, while the corrosion on the black pearl 2000 starts on the particle surface. XRD results show that the 0 0 2 and 10 peaks of the XC72-based samples are initially sharp, but then broaden during the corrosion process. For black pearl 2000-based samples, the 0 0 2 and 10 peaks all became broader during the corrosion process. The results provide guidelines for modifying carbon black as catalyst supports to achieve a higher durability.

1. Introduction

With the pressing environmental requirements on reducing automobile emissions, finding an alternative automotive propulsion system with fewer emissions than an internal combustion engine has become more urgent than ever. Recently, rising oil prices have accelerated efforts and exploration – not only for emissions, but also for higher energy efficiency and the use of alternative energy. PEFCs are the best candidates for automobile propulsion due to their ultimate cleanness – zero emissions, low operating temperatures (e.g. 80 °C), high-energy efficiency (i.e. >65% [1]), and the use of alternative fuels (i.e. hydrogen). As PEFCs are being driven toward commercialization, the challenge of high durability has emerged, while PEFCs are still being pushed to have higher performance and lower cost. High durability is not only a requirement for PEFC applications in automobiles; it is also the most effective way to reduce the cost of PEFCs. PEFC performance loss during long-term operations under steady and dynamic conditions has been attributed to the corrosion of carbon blacks (as catalyst supports), the degradation of Pt and Pt alloy catalyst nanoparticles, the Nafion ionomer network inside catalyst layer, and the Nafion membrane [2–7].

In PEFCs, platinum nanoparticles and their alloys are usually dispersed on porous carbon black (e.g., Vulcan XC72) to function as PEFC anode and cathode catalysts [8,9]. Carbon black supports are easily oxidized when the potential is greater than 0.55 V [10,11]. This corrosion is accelerated when Pt nanoparticles exist on the surface of carbon blacks. Thus, carbon corrosion contributes to a great performance loss in PEFCs, and particularly when PEFCs are operating under an automobile driving cycle [12], both anode and cathode experience a sharp potential spike as high as 1.20 V (*vs.* saturated hydrogen electrode) [13], causing severe carbon corrosion.

The corrosion of carbon supports has been investigated by several groups [14–19], however, these investigations focused only on the carbon corrosion phenomena in a fuel cell environment or in a simulated fuel cell environment. Little work has been reported on the corrosion mechanism of carbon black supports in PEFCs, although it is speculated that the carbon corrosion starts from the center of an XC72 carbon black particle. The current approaches for dealing with the corrosion of catalyst carbon supports is (1) to find alternative catalyst support materials (i.e. metal oxides and metal carbides), (2) to use graphite material as the catalyst support, and (3) to improve current widely used Vulcan XC72 carbon black through surface modification [20–21]. Most metal oxides have low electronic conductivity, while both metal oxides and metal carbides have high density, which makes them hard to disperse in a catalyst ink. The graphite materials are very hydrophobic, which makes it difficult for them to disperse the Pt and Pt alloy nanoparticles. It appears that the carbon blacks are still the best catalyst support so far in terms of the dispersion of Pt and Pt alloy catalyst nanoparticles, density, hydrophilicity, and electronic conductivity. Therefore, modification of either the surface or bulk of the carbon black sup-

* Corresponding author. Tel.: +1 317 274 8850.
E-mail address: jianxie@iupui.edu (J. Xie).

0254-0584/$ – see front matter © 2010 Elsevier B.V. All rights reserved.
doi:10.1016/j.matchemphys.2010.05.055

Table 1
Weight loss and crystal properties of the samples.

Sample	Temperature (°C)	Time (h)	Weight loss (%)	Average particle size (nm)[a]	β_{002}[b]	β_{10}[c]
XC72				48.50	6.45	5.39
XC800-1	800	1	15.52	49.21	4.21	3.65
XC800-3	800	3	28.43	49.43	5.01	2.86
XC1000-1	1000	1	28.9	49.59	5.41	4.97
XC1000-3	1000	3	67.12	48.71	9.76	6.77
BP2000				32.20	9.01	4.42
BP800-1	800	1	32.54	19.75	11.36	5.74
BP800-3	800	3	54.82	18.38	15.23	
BP1000-1	1000	1	100			

[a] Average particle size of five carbon black particles in TEM micrograph.
[b] The full width at half maximum of the diffraction peak.
[c] The full width at half maximum of the diffraction peak.

ports on to enhance the corrosion resistance is the realistic choice for improving the durability of PEFCs. The carbon corrosion can be deterred by applying either the surface modification if the corrosion starts on the surface, or by applying the bulk modification (i.e. increase the degree of graphitization) if the corrosion starts from the center of a carbon black particle.

Investigation of the corrosion mechanism of a carbon support in a membrane electrode assembly (MEA) of PEFCs is difficult because several parallel degradation processes are occurring (Pt and alloy catalyst nanoparticles, ionomer degradation, membrane degradation and carbon corrosion). Decoupling the carbon corrosion from the experimental data is difficult due to the complexity of the PEFC degradation. Since our interest is to understand how the carbon black is corroded (i.e. from the surface or from the bulk), the steam etching approach was used in our study of the carbon corrosion because there are always water films either inside the Nafion ionomer network or directly on carbon surface during the PEFC operation. The carbon blacks that came into contact with high temperature steam then subject to accelerated corrosion. The weight loss, morphology, and structural changes of carbon blacks were examined using XRD, SEM, and TEM.

2. Experimental

2.1. Corrosion process for carbon blacks

Two different carbon blacks, a high-surface area (1500 $m^2\,g^{-1}$) black pearl 2000 (BP2000), and a low-surface area (254 $m^2\,g^{-1}$) carbon black Vulcan XC72 (XC72) were used. Both XC72 and BP2000 were as received from Cabot (Billerica, MA). A furnace with a gas inlet and an exit was used for the steam etching experiment. The aggregates of these carbon black powders were milled before etching experiments. The milled carbon black powders were placed into the tube furnace and then were purged with nitrogen while the temperature was increased through programmed heating at a heating rate 5 °C min^{-1}. The steam was introduced into the furnace when the furnace reached the desired temperatures and the steam continued flowing through the furnace for a certain length of time. The flow rate of steam is 0.5 $cm^3\,min^{-1}$ (water) and the flow rate is the same in all experiments. The steam etched products were labeled as XC*x*–*y* or BP*x*–*y*, where *x* represents the steam etched temperature and *y* is the steam etched time, while XC and BP represent carbon black XC72 and black pearl 2000, respectively.

2.2. Characterization of steam etched carbon blacks

The mass of the carbon blacks was measured before and after the steam etching experiment to determine the weight loss of the carbon blacks in the steam etching process. The crystal structures of the fresh and etched carbon blacks were analyzed using powder X-ray diffraction (XRD). The XRD diffractometer utilized Cu Kα radiation (40 kV and 30 mA) and the data were collected as continuous scans, with a step of 0.02° (2θ) and a scanning rate of 2° (2θ) min^{-1} between 10 and 90° (2θ). The morphologies of the steam etched samples were examined using Hitachi S-4800 scanning electron microscope (SEM) and Philip Tecnai 20 transmission electron microscope (TEM).

3. Results and discussion

The principal objective of this study is to investigate the carbon black corrosion process using the steam etching approach and to provide a model system for studying the catalyst support corrosion mechanism in PEFCs. The weight loss of the two different carbon blacks in Table 1 suggests that XC72 and BP2000 may go through different corrosion processes. Understanding these carbon black corrosion processes will help to study the PEFC degradation mechanism.

The weight loss and the calculated full width at half maximum of the diffraction peak of carbon black samples are summarized in Table 1. For both XC72 and BP2000, the weight loss increases with the steam etching temperatures and times. Compared with XC72 samples, the BP2000 carbon blacks show a larger weight loss than the XC72 samples at the same temperature and etching time. The weight loss of the XC1000-3 is 67.12%, while the weight loss BP1000-1 is 100%. In the experimental observation, all BP2000 samples were completely gone after 1 h of steam etching at 1000 °C. The weight loss of carbon blacks after steam etching is a direct indication of carbon black corrosion: the higher the weight loss, the greater the corrosion. The difference in the weight loss of XC72 and BP2000 suggests that these two carbon blacks may have different corrosion processes, which could be associated with their chemical and morphologic structure (i.e. degree of graphitization, particle size, surface area, pore structure, etc.). The major difference between XC72 and BP2000 is their surface area, 254 $m^2\,g^{-1}$ *vs.* 1500 $m^2\,g^{-1}$ (XC72 *vs.* BP2000). Since the steam etching is a surface reaction, it can be hypothesized that the higher weight loss of BP2000 samples in comparison with the XC72 samples under the same etching conditions is attributed to the higher surface area of BP2000.

TEM micrographs of XC72 samples are shown in Fig. 1. A fresh XC72 carbon black particle is shown in Fig. 1(a) and (b). The characteristic feature of the XC72 particle is that the graphite layer planes are concentrically parallel to each other toward the center, which is similar to the pattern of a fingerprint. Close examination of Fig. 1(b) reveals that the graphite layer plane is concentrically parallel but in a more disorderly arrangement. This feature matches the carbon black microstructure model proposed by Heckman [22]. Fig. 1(e) is the micrograph of XC72 carbon black sample after 3 h of etching. It can be clearly seen that the center of the carbon black particle became brighter (as the arrow points to in Fig. 1(e)) than the rest of particle, consistent with the interpretation that the particle center has experienced greater mass loss than the rest of the particle. Comparing that with the micrograph of a fresh XC72 in Fig. 1(a) and (b), it appears that a hole begins to emerge after steam etching for 3 h. It can be seen in Fig. 1(f), which is a higher magnification micrograph of Fig. 1(e) that the center of the XC72 particle was significantly corroded, and the carbon layer planes are more disorderly when compared with Fig. 1(b). In addition, in Fig. 1(f), some carbon layer planes on the outermost surface of the carbon black sphere became cracked. However, through a comparison of micrograph Fig. 1(a), (c), and (e), it can be clearly seen that the carbon black particle size remains almost the same after steam etching,

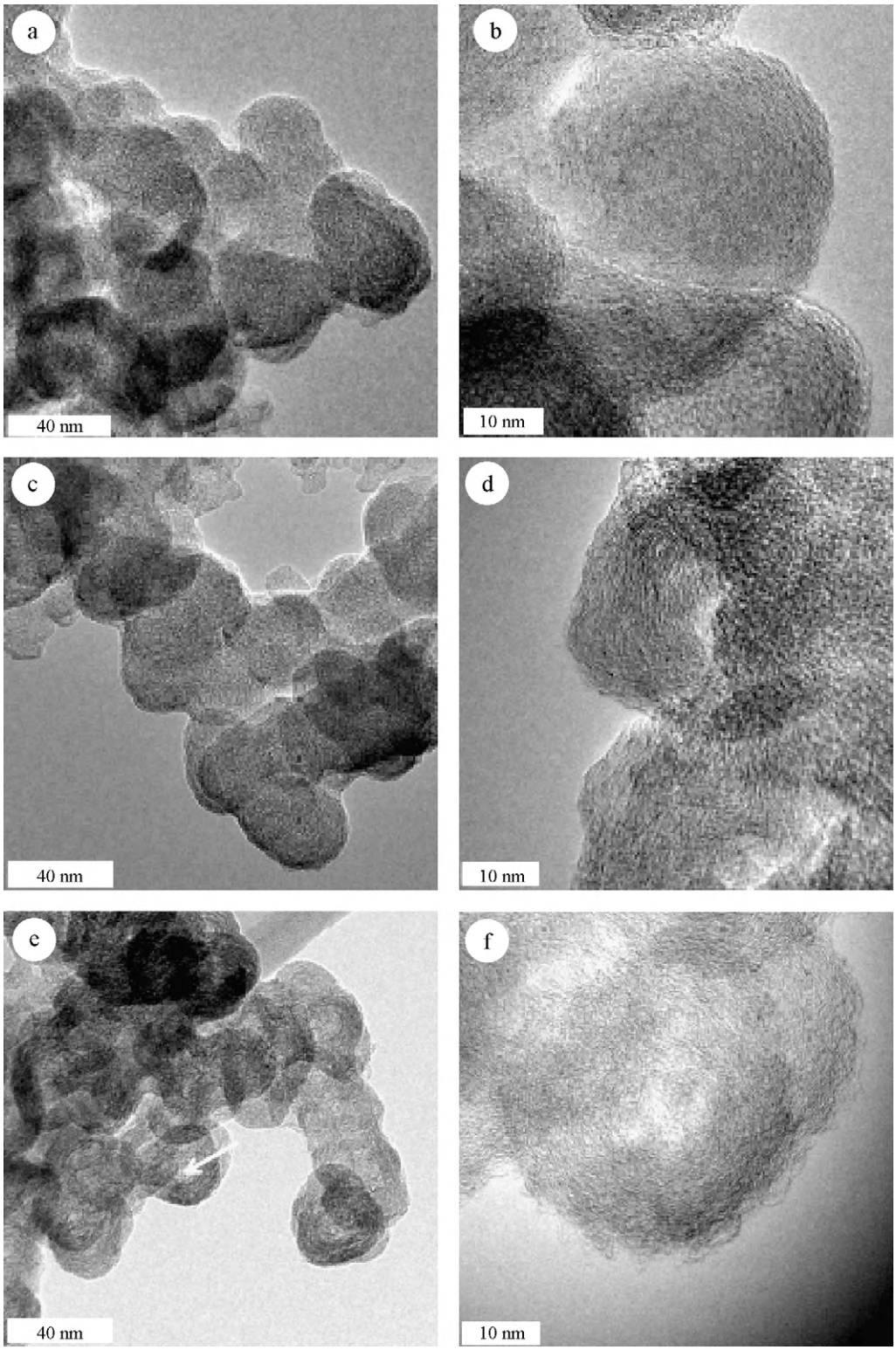

Fig. 1. TEM micrographs of the steam etched samples. (a and b) XC72; (c and d) XC721000-1; (e and f) XC721000-3; b, d, and e are the higher magnification micrographs of a, c, and d.

even for 3 h at 1000 °C. Apparently, the strongest corrosion occurs at the center of the XC72 particle rather than on the surface.

The micrographs of XC72 etched for 1 h are shown in Fig. 1(c) and (e). It can be seen that no significant morphologic changes occur in comparison with XC72 etched for 3 h under 1000 °C, but the surface becomes some smooth after etching. However, from Table 1, it can be seen that the weight loss after 1 h of etching is 28.9%. Combining the TEM micrographs and the weight loss in Table 1, it is clear that that major corrosion occurred at the center of the XC72 particle with some minor corrosion on the surface of the carbon particle to remove some amorphous structured carbon blacks filaments, which will be explained in detail by the XRD spectra.

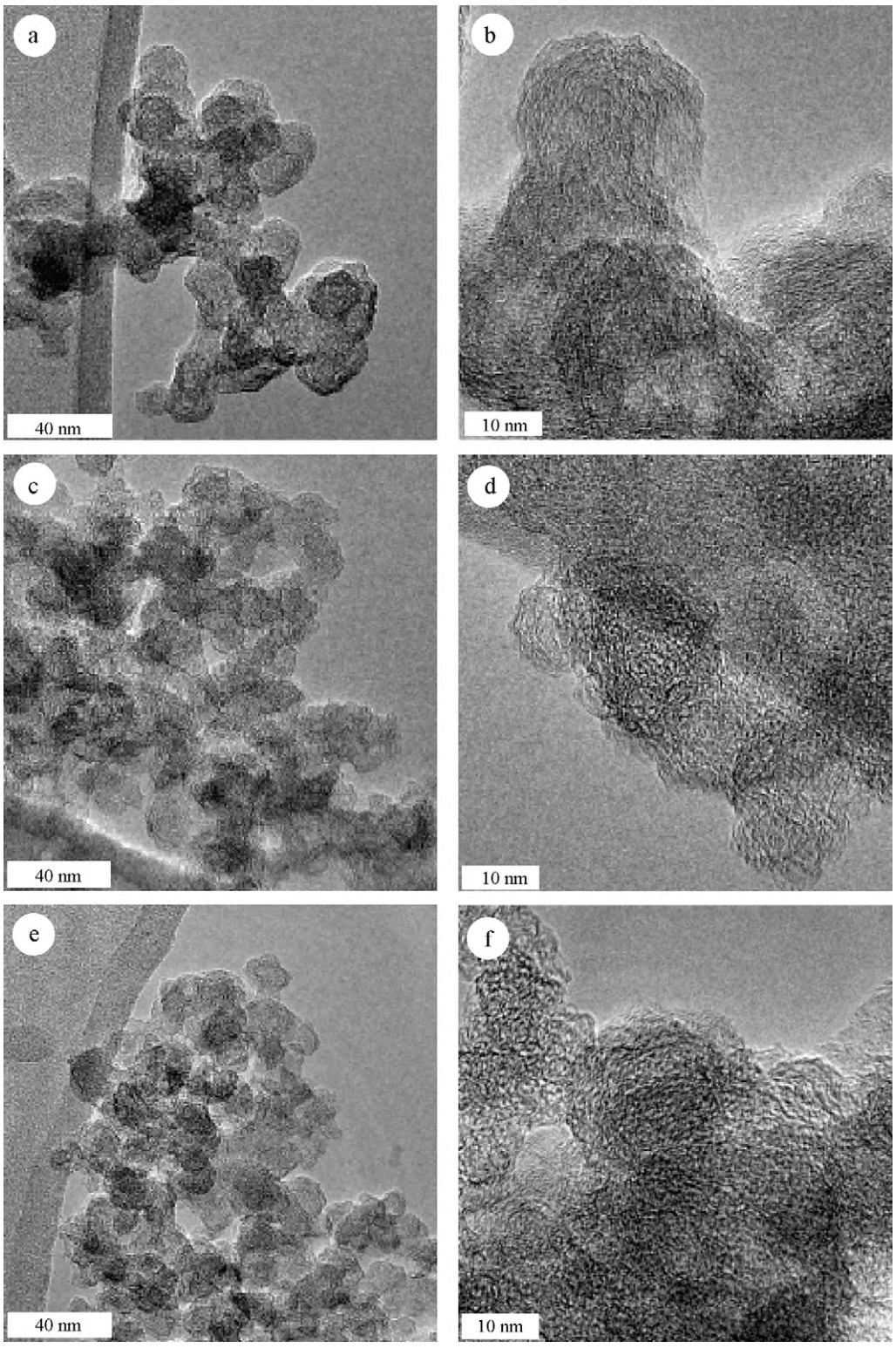

Fig. 2. TEM micrographs of steam etched samples. (a and b) BP2000; (c and d) BP800-1; (e and f) BP800-3.

The TEM micrographs of BP2000 are shown in Fig. 2. It can be clearly seen that the corrosion feature of BP2000 is different from that of the XC72 samples. The significant difference between the fresh XC72 and BP2000 is that the BP2000 graphite layer planes are not as concentrically parallel to each other toward the center as the XC72 counterpart. The disorderly portion found in a BP2000 particle is far more prevalent than that in an XC72 particle (compare Fig. 1(a) and (b) with Fig. 2(a) and (b)). No bright features are apparent in the center of the BP2000 particles after etching for 3 h at 800 °C (in Fig. 2), although the weight loss of the BP800-3 is 54.82% (Table 1). Through comparison of Fig. 2 (a), (c), and (e) and Table 1, it can be seen that the particle size significantly decreases with the etching time. The particle size change can also be seen from the SEM micrographs in Fig. 3 and from the data present in Table 1. The weigh

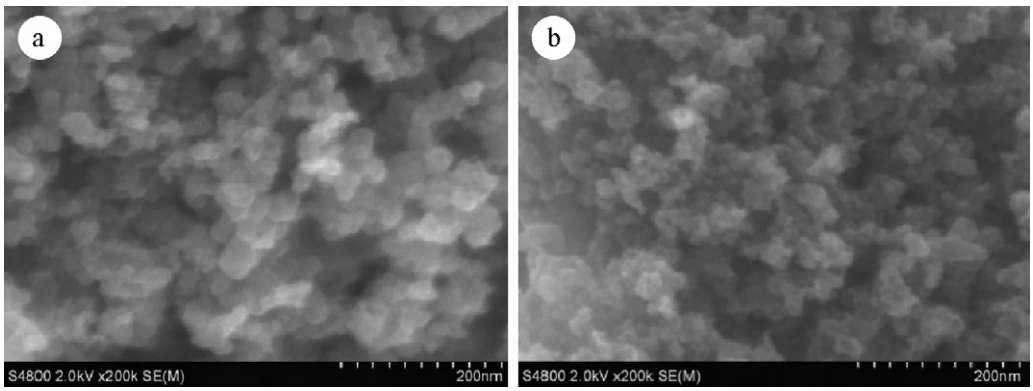

Fig. 3. SEM micrographs of the samples. (a) BP2000; (b) BP800-3.

loss of BP1000-1 is 100%. Compared to XC72 carbon blacks, BP2000 carbon blacks show a larger weight loss under the same conditions. Therefore, it can be concluded that BP2000 is more easily corroded than XC72 under equivalent conditions. The lower corrosion resistance of BP2000 can be attributed to two factors: (1) the surface area of the BP2000, which is 1500 $m^2\,g^{-1}$, much larger than that of the XC72 254 $m^2\,g^{-1}$, and (2) the particle size of BP2000, which is smaller than that of the XC72 (see Figs. 1(a) and 2(a)). In addition, the microstructure of BP2000 is less ordered and the carbon layer planes are less uniform in structure, unlike XC72, which has a more dense carbon layer plane structure as suggested by the values of full width at half maximum in Table 1, and a more ordered structure in the particle center.

The different corrosion processes of XC72 and BP2000 carbon blacks originate from their differences in the structure of the graphitic carbon layers. XC72 has a more dense graphitic structure at the surface (compare the β_{002} and β_{10} in Table 1 for XC72 and BP2000 and Fig. 1(a) and (b) with Fig. 2(a) and (b)) and a more disordered structure in the particle center, thus the corrosion process begins from the center rather than from the surface. That the corrosion mainly occurs at the particle center is suggested by the fact that particle size remains almost the same, even after 3 h of etching. But for BP2000, the carbon layer planes structure is uniform and no significant difference appears between the surface graphitic layers and center graphitic layers. Therefore, the BP2000 corrosion begins on the surface, and particle size decreases with etching time.

The X-ray diffraction patterns for the XC72 and BP2000 carbon black samples are shown in Figs. 4 and 5. For graphite, the 0 0 2 peak is expected at around 26.38°, the 100 peak at 42.22°, and the 101 peak at 44.39° [23]. For the amorphous carbon black samples, a broad peak corresponding to the 0 0 2 reflection is shifted downwards and is seen around 22.5°. The shift of the 0 0 2 reflection to lower values leads to the larger d_{002} suggesting a more amorphous phase in the XC72 carbon blacks. Furthermore, for turbostratic two-dimensional ordering, the 100 and 101 peaks merge into a broad 10 peak around 43°. From Fig. 4, it can be seen that the XC72 steam etched carbon blacks at 800 °C and the 0 0 2 and 10 peaks became sharper as the etching time increased. The crystallite size also increased because a broader peak is usually associated with a smaller crystallite size [24]. When the etching temperature increased to 1000 °C, however, the 0 0 2 and 10 peaks of the samples initially became sharper and then became broad again. The crystallites size of these samples also increased initially and then deceased as the etching time increased. For the BP2000 samples, the 0 0 2 and 10 peaks became broader with the increase in etching time. The crystallites size of these samples also decreased.

Carbon black is one of the classes of carbon materials that have a form different from the forms of diamond, coke, charcoal and graphite. Carbon blacks consist mostly of spherical and ellipsoidal particles [23]. These particles have both amorphous and crystalline substructures. They may be visualized as being composed of more or less oriented graphitic layer planes. They exhibit various extents

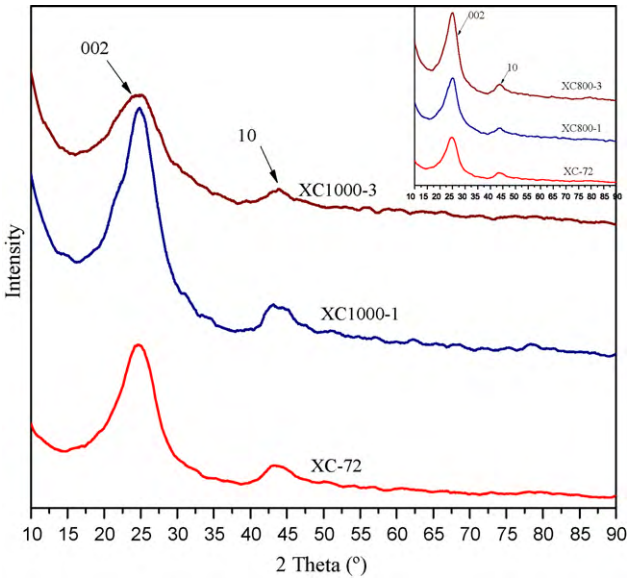

Fig. 4. XRD spectra of XC72 and XC72 derived samples.

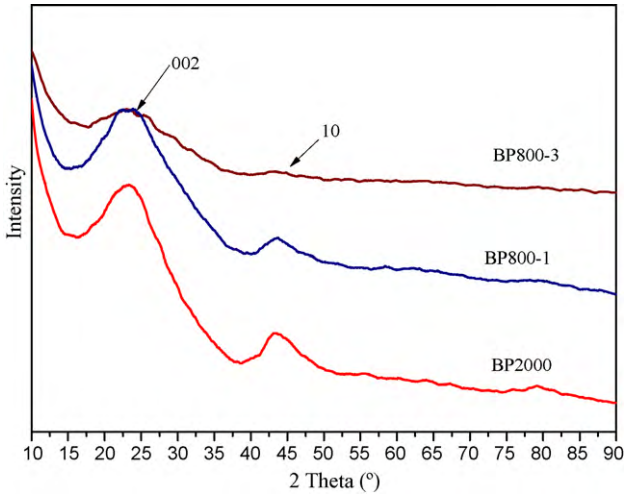

Fig. 5. XRD spectra of BP2000 and BP2000 derived samples.

of electrical conductance because of their predominant graphite-like structures. They have defects, dislocations, and discontinuities at the edges of the layer planes. These defects and the amorphous part of carbon black particles were first corroded during the steam etching process, and the crystalline substructures remained. Then, the crystalline substructures were corroded in the steam etching process. This is probably the reason that the 0 0 2 and 10 peaks of the XC72 samples initially became sharper before becoming broad again. As for the BP2000 samples, the corrosion process begins on the particle surface because of its high-surface area, small particle size, and more ordered carbon layer plane structure. This is probably the reason the 0 0 2 and 10 peaks became broader as the etching time increased.

4. Conclusions

The corrosion of carbon blacks of XC72 and BP2000 was carried out using steam etching under different conditions, and the corrosion processes were clearly observed for XC72 and BP2000 carbon blacks. For XC72 carbon blacks, the corrosion begins from the center of the particle while the corrosion starts on the surface of particle for BP2000 carbon blacks. The morphology, and specifically, the carbon layer plane structure of carbon black particles, is the major factor in determining the corrosion process. The higher the surface area, the smaller the particle size and the less dense the carbon layer plane structure is, which allows BP2000 to be more easily corroded than XC72.

As shown in the XRD spectra, the different structures of the carbon layer planes also determine the different microcrystallite structural changes during the corrosion process. For XC72-based carbon blacks, the 0 0 2 and 10 peaks first became sharper and then became broad again during steam etching, which corresponds with the idea that the defects and the amorphous phase are corroded away from the carbon blacks, and then the microcrystallites are further corroded. For BP2000 carbon blacks, the 0 0 2 and 10 peaks all became broader during the corrosion process, suggesting a more amorphous phase in the BP2000 carbon blacks after etching. The findings of the dependence of the corrosion process on the microstructure of carbon blacks provide guidelines for developing novel catalyst supports with high durability. To increase corrosion resistance for XC72-based catalyst supports, the bulk structure of the particles needs to be improved so that the each graphite layer plane is concentrically parallel like a perfect fingerprint. On the other hand, surface protection for BP2000-based catalyst supports is needed to increase corrosion resistance.

Acknowledgements

The authors would like to thank F. Vincent Hernly at earth science department of Indiana University-Purdue University Indianapolis for assistance on XRD measurements and analysis.

References

[1] A. Gasteiger, S.S. Kocha, B. Sompalli, F.T. Wagner, Appl. Catal. B: Environ. 56 (2005) 9.
[2] J.R. Dahn, D.A. Stevens, Carbon 43 (2005) 179.
[3] H. Tang, M. Pan, F. Wang, P.K. Shen, S.P. Jiang, J. Phys. Chem. B 111 (2007) 8684.
[4] H.A. Gasteiger, J.E. Panels, S.G. Yan, J. Power Sources 127 (2004) 162.
[5] K.G. Gallagher, D.T. Wong, T.F. Fuller, J. Electrochem. Soc. 155 (2008) B488.
[6] A.C. Fernandes, E.A. Ticianelli, J. Power Sources 193 (2009) 547.
[7] S. Rojas, D. Fuente, M. Huerta, P. Terreros, M.A. Pena, J.L.G. Fierro, Carbon 2006 (2006) 1919.
[8] A. Guha, W.J. Lu, T.A. Zawodzinski, D.A. Schiraldi, Carbon 45 (2007) 1506.
[9] S. Gottesfeld, T.A. Zawodzinski, Polymer Electrolyte Fuel Cells in Advances in Electrochemical Science and Engineering, Wiley and Sons, New York, 1998, p. 102.
[10] K.H. Kangasniemi, D.A. Condit, T.D. Jarvi, J. Electrochem. Soc. 151 (2004) E125.
[11] K. Kinoshita, Carbon: Electrochemical and Physicochemical Properties, John Wiley, 1988, p. 318.
[12] R.L. Borup, J.R. Davey, F.H. Garzon, D.L. Wood, M.A. Inbody, J. Power Sources 163 (2006) 76.
[13] J. Xie, Oxygen reduction on Pt and Pt alloys: catalyst degradation in polymer electrolyte fuel cells, in: T. He (Ed.), Catalysts for Oxygen Electroreduction—Recent Developments and New Directions, Transworld Research Network, India, 2009, p. 661.
[14] M. Cai, M.S. Ruthkosky, B. Merzougui, S. Swathirajan, M.P. Balogh, S.H. Oh, J. Power Sources 160 (2006) 977.
[15] J. Wang, G. Yin, Y. Shao, S. Zhang, Z. Wang, Y. Gao, J. Power Sources 171 (2007) 331.
[16] A.S. Arico, A. Stassi, E. Modica, R. Ornelas, G.I. atto, E. Passalacqua, V. Antonucci, J. Power Sources 178 (2008) 525.
[17] Y. Shao, G. Yin, Y. Gao, P. Shi, J. Electrochem. Soc. 153 (2006) A1093.
[18] W. Bi, T.F. Fuller, J. Electrochem. Soc. 155 (2008) B215.
[19] A.P. Young, J. Stumper, E. Gyenge, J. Electrochem. Soc. 156 (2009) B913.
[20] Y. Shao, J. Wang, R. Kou, M. Engelhard, J. Liu, Y. Wang, Eletrochim. Acta 54 (2009) 3109.
[21] J. Xie, F. Garzon, T. Zawodzinski, W. Smith, J. Electrochem. Soc. 151 (2004) A1084.
[22] F.A. Heckman, Rubber Chem. Technol. 37 (1969) 1245.
[23] N. Krishnankutty, M.A. Vannice, Chem. Mater. 7 (1995) 754.
[24] N. Iwashuta, C.R. Park, H.F. Jimoto, M. Shiraishi, M. Inagaki, Carbon 44 (2004) 701.